10.1161/CIRCULATIONAHA.118.039022

Mapping and Ablation of Ventricular Fibrillation Associated with Early Repolarization Syndrome

Running Title: *Nademanee et al.; VF Ablation in Early Repolarization Syndrome*

Koonlawee Nademanee, MD[1,2]; Michel Haissaguerre, MD[3]; Mélèze Hocini, MD[3]; Akihiko Nogami, MD[4]; Ghassen Cheniti, MD[3]; Josselin Duchateau, MD[3]; Elijah R Behr, MD[5]; Magdi Saba, MD[5]; Ryan Bokan, BS[6]; Qing Lou, PhD[6]; Montawatt Amnueypol, MD[2]; Ruben Coronel, MD, PhD[7]; Apichai Khongphatthanayothin, MD[1]; Gumpanart Veerakul, MD[8]

[1]Chulalongkorn University, Bangkok Thailand; [2]Pacific Rim Electrophysiology Research Institute at Bumrungrad Hospital, Bangkok, Thailand and Los Angeles, CA; [3]IHU Liryc, Electrophysiology and Heart Modeling Institute, Foundation Bordeaux Université, Pessac-Bordeaux, Bordeaux, France; [4]University of Tsukuba, Tsukuba, Japan; [5]Cardiology Clinical Academic Group, Institute of Molecular and Clinical Sciences, St George's, University of London, and St. George's University Hospitals NHS Foundation Trust London, UK; [6]CardioInsight Technologies, Medtronic, Minneapolis, MN; [7]Dept. Exp. Cardiology, Academic Medical Center, Amsterdam, The Netherlands; [8]Bhumibol Adulyadej RTAF Hospital, Bangkok, Thailand

Address for Correspondence:
Koonlawee Nademanee, MD
Chulalongkorn University
185/19 (16R) Ratchadamri road. Pathumwan
Bangkok, Thailand 10330
Tel: +1-310-309-7260
Email: wee@pacificrimep.com

Abstract

Background: We conducted a multicenter study to evaluate mapping and ablation of ventricular fibrillation (VF) substrates or VF triggers in early repolarization syndromes (ERS) or J-wave syndrome (JWS).

Methods: We studied 52 ERS patients (4 females; median age, 35 years) with recurrent VF episodes. Body-surface electrocardiographic imaging (ECGI) along with endocardial and epicardial electroanatomic mapping of both ventricles were performed during sinus rhythm and VF for localization of triggers, substrates, and drivers. Ablations were performed on:1) VF substrates defined as areas that had late depolarization abnormalities characterized by low voltage fractionated late potentials and 2) VF triggers.

Results: Fifty-one of the 52 patients had detailed mapping which revealed two phenotypes: 1) Group 1 had late depolarization abnormalities predominantly at the right ventricular (RV) epicardium (n=40); and 2) Group 2 had no depolarization abnormalities (n=11). Group 1 can be subcategorized into 2 groups: Group 1A included 33 ERS patients with Brugada ECG pattern, and Group 1B included 7 ERS patients without Brugada ECG pattern. Late depolarization areas co-localize with VF driver areas. The anterior RV outflow tract (RVOT)/RV epicardium and the RV inferior epicardium are the major substrate sites for Group 1. The Purkinje network is the leading underlying VF trigger in Group 2 that had no substrates. Ablations were performed in 43 patients: 33 and 5 Group 1 patients had only VF substrate ablation and VF substrates plus VF trigger, respectively (mean 1.4 ± 0.6 sessions); 5 Group 2 patients and 1 without group classification had only Purkinje VF trigger ablation (mean 1.2 ± 0.4 sessions). Ablations were successful in reducing VF recurrences ($p<0.0001$). After follow-up of 31 ± 26 months, 39 (91%) had no VF recurrences.

Conclusions: There are 2 phenotypes of ERS/JWS: 1) one with late depolarization abnormality as the underlying mechanism of high amplitude J-wave elevation that predominantly resides in the RVOT and RV inferolateral epicardium, serving as an excellent target for ablation; and 2) the other with pure ERS devoid of VF substrates, but with VF triggers that are associated with Purkinje sites. Ablation is effective in treating symptomatic ERS/JWS patients with frequent VF episodes.

Key Words: Ventricular Fibrillation, Early Repolarization syndrome, J-wave syndrome, catheter ablation

Non-Standard Abbreviations and Acronyms

VF = Ventricular fibrillation.
ERS = Early repolarization syndrome.
BrS = Brugada syndrome
JWS = J-wave syndrome
RVOT = Right ventricular outflow tract
RV = Right ventricle

Clinical Perspective

What is new?

- In highly symptomatic early repolarization syndrome (ERS) patients, we found 2 distinct phenotypes: those with late depolarization abnormalities (Group 1), and those without late depolarization abnormalities (Group 2).
- Group 1 patients can be subcategorized into 2 groups: 1) those with concomitant Brugada ECG pattern (Group 1A), and 2) those without Brugada ECG pattern (Group 1B).
- Catheter ablation of the arrhythmogenic substrates with late depolarization abnormalities is effective in preventing VF recurrence in Group 1 patients and ablation of VF triggers emanating from the Purkinje system is also effective in treating Group 2 patients.

What are the clinical implications?

- Our data strongly suggest that depolarization abnormalities are the main underlying pathophysiologic mechanisms of Group 1 ERS patients while repolarization abnormalities may be the mechanism responsible in Group 2 ERS patients.
- Catheter ablation appears to be safe and effective therapeutic modality for symptomatic ERS.
- Our study findings increase the understanding of the pathophysiology of ERS; further research to identify the cause of these depolarization abnormalities is warranted.

Introduction

Early repolarization (ER), highly prevalent in young populations, was initially thought to be a benign electrocardiographic (ECG) finding for several decades.[1] However, a decade ago, several studies showed that ER, characterized by high amplitude J wave and horizontal/descending ST elevation in the inferior or lateral leads or both, is associated with an increased risk of ventricular fibrillation (VF) and sudden cardiac death.[2-4] The discovery of the inferolateral ER marker as a risk for sudden death in patients who are otherwise healthy and have no structural heart disease, known as early repolarization syndrome (ERS), has spurred concern, awareness, and interest among electrophysiologists and cardiologists.

Together with the Brugada syndrome (BrS), the ERS has been included in the family of the J-wave syndrome (JWS) as distinct electrocardiographic phenotypes that affect the junction (J) between the QRS complex and the ST segment in inferolateral leads. Based on studies in the canine wedge preparation, the underlying electrophysiologic mechanism of the syndrome was initially attributed to heterogeneity of the voltage gradient during repolarization across the ventricular wall.[5] However, based on emerging evidence the role of an arrhythmogenic substrate in BrS[6], one must explore the possibility that alternative mechanisms, including conduction abnormalities (e.g., local depolarization abnormality or a combination of both repolarization and depolarization abnormalities) play a role in the pathophysiology of the ERS.[6]

Currently, ERS treatment options are limited to 2 established modalities: 1) pharmacologic treatment with quinidine for long-term prevention of recurrent VF and isoproterenol for acute treatment of patients who have suffered implantable cardioverter-defibrillator (ICD) storm from frequent VF episodes; and 2) ICD for sudden death prophylaxis in patients who have suffered life-threatening ventricular tachyarrhythmias. Thus far, there have

been a few case reports of successful catheter ablation of VF triggers for treatment of ERS patients with electrical storm.[7-9] Better characterization of the arrhythmogenic substrate and VF drivers in ERS are needed to identify targets for ablation therapy. Thus, we carried out a multi-center collaborative study aiming to map patients who experienced frequent VF episodes associated with inferolateral ER, to determine the role of catheter ablation for treatment of symptomatic ERS patients.

Methods

We declare that all supporting data are available within the article and its online supplementary files.

Study Population

We retrospectively studied symptomatic ERS patients who either survived recurrent VF episodes or had cardiac or unknown syncope or agonal respiration during sleep. These patients were recruited from 4 institutions in 5 locations, Chulalongkorn University and Pacific Rim Electrophysiology Research Institute (Bangkok and Los Angeles); University of Bordeaux, France; University of Tsukuba, Japan; and St. George's University Hospitals NHS Foundation Trust, United Kingdom (Table 1). All patients underwent echocardiography or magnetic resonance imaging (MRI) examination to exclude structural heart disease. Patients with inferolateral JWS without concomitant spontaneous Brugada ECG pattern also underwent provocation test with sodium channel blockers (ajmaline, procainamide, and pilsicainide). Patients with combined inferolateral J wave and Brugada patterns, either spontaneously or after sodium channel blockade, were included. We excluded patients with severe anoxic brain damage from prior cardiac arrests and those with structural heart diseases or precipitating factors

that could give rise to ER pattern or VF (i.e., ischemia, coronary vasospasm, drug abuse, and hyperkalemia). Only 32 patients (62%) had a complete genetic testing. The study was approved by the respective institutional review boards and all patients signed an informed consent.

Electrophysiologic Studies and Mapping of the VF Substrate

Invasive Mapping

Detailed epicardial and endocardial electroanatomic mapping was performed during sinus rhythm using the Carto Navigation System (Biosense Webster, Inc., Diamond Bar, CA). We paid specific attention to sites with activation times coinciding with the electrocardiographic J wave. The EGMs occurring within (and possibly after) the J wave were considered as belonging to depolarization if they were sharp and in temporal and spatial continuity with the depolarization field mapped at the end of the QRS complex. An abnormal EGM was defined as a bipolar EGM that had: 1) low voltage (≤1 mV), and 2) split EGM or fractionated EGM lasting ≥70 ms. Such abnormal areas were tagged and defined as "VF ventricular substrate," as described previously.[10,11] The European and Thai study sites used ajmaline (1mg/kg doses up to 100 mg) to unmask areas with abnormal electrogram, whereas the Japanese and the US sites used pilsicainide and procainamide for the same purpose. None of the sites used warm-saline during mapping of the VF substrates.

Programmed electrical stimulation for VF induction (S1-S1 at 600, 500, and 400 ms and up to triple ventricular extra-stimuli) was performed via the quadripolar catheter in the apex of the right ventricle (RV) or its outflow tract (RVOT). Cardioversion/defibrillation was performed to restore sinus rhythm after 10 seconds of VF.

Non-invasive Mapping Using Electrocardiographic Imaging

Patients studied at Bumrungrad Hospital, Bangkok, Thailand and at Hôpital Cardiologique du Haut Lévèque, Bordeaux–Pessac, France, between January 2016 and June 2018, also underwent the electrocardiographic imaging (ECGI) mapping procedure with the CardioInsight system (Medtronic, St. Paul, MN). ECGI methodology has been described.[12,13] Patient-specific geometry and body surface ECG recordings were acquired through a 252 electrode-vest attached to the skin. The chest-heart geometry was created prior to the procedure using a low-dose computed tomography to localize vest electrode positions relative to the ventricular epicardial surface. A 3D model of the heart was created using dedicated software (CardioInsight, Medtronic, St. Paul, MN).

The patients were then transferred to the electrophysiology laboratory while wearing the vest, which remained in the same position during the invasive mapping and ablation procedure. Body surface ECG recordings from the vest electrodes were acquired before and during the invasive mapping procedure. Based on the inverse solution, the system automatically displays epicardial wavefront patterns on the 3D reconstruction of the patient's heart. In this manner, activation mapping was performed during spontaneous or induced VF. After adequate filtering, dynamic wavefront propagation maps were generated using phase mapping. The wavefront patterns were displayed on the epicardial surface (patterns detailed below), serving as VF maps.[12,13]

We analyzed the VF maps during an initial organized period of VF (the initial 5 seconds), as previously described; cardioversion was performed if VF lasted > 10 seconds.[14] VF drivers were defined as either focal breakthroughs when centrifugal activation originated from a given site or full re-entrant activity with a high activation frequency. The wavefront maps, derived

from phase mapping, display the electrical wavefront at the pi/2 phase value of each ECGI-calculated unipolar EGM, serving as a surrogate for local activation. Focal breakthroughs are detected when this wavefront emerges from a point and activates a portion of the heart. Rotations are detected when the rotational core, or singularity point, of a rotating wavefront is within a 2.5-cm area for ≥1.5 rotations. We then created spatiotemporal density maps displaying the number, location, and spatial extent (of reentry trajectories) of VF drivers, and the colored hexagon represents the number and location of epicardial focal breakthrough (see below).

Mapping of VF Triggers

We aimed to identify the site of earliest activation relative to the onset of the QRS complex of the premature ventricular contraction (PVC) triggering VF. Obviously, this was possible only when these PVCs were frequent enough to map. An initial sharp potential (<10 ms in duration) preceding the larger and slower ventricular electrogram (EGM) by <15 ms during sinus rhythm represented a peripheral Purkinje fiber, whereas longer intervals indicated proximal Purkinje fascicle activation. A Purkinje potential preceding a spontaneous ventricular activation was interpreted as an indication of a Purkinje origin of that premature beat.

Ablation Protocol and Clinical Endpoints

Ablations were invariably performed with irrigated-tip catheters, using contact-force catheters when these became available in 2013. We used a contact force >5 g at all target sites; and RF power was titrated between 20-50 Watts depending on the contact force, guided by close continuous observation of the voltage reduction of the late fractionated electrogram and the disappearance of mid and late components of the fractionated potentials during ablation, as previously described.[11]

The ablation targets were: 1) VF trigger areas as defined above; 2) VF substrates, defined as areas that harbor abnormal ventricular EGMs based solely on electroanatomical mapping; 3) or both. The ablation endpoint for VF triggers was the elimination of the PVC-VF triggers; for VF substrates, it was the elimination of all abnormal late fractionated EGMs. Non-inducibility of sustained ventricular arrhythmias was not our ablation end point, although it was carried out at the discretion of operators in the majority of our patients. We defined inducible ventricular tachycardia (VT)/VF as induced VT/VF lastitng ≥10 seconds.

All patients were followed 1 month after the ablation session and every 3 months thereafter. Our clinical endpoints were 1) death and 2) the long-term incidence of VF episode(s), monitored by ICD interrogation.

Statistical Analysis

Student t-test and Wilcoxon rank-sum test for continuous variables and Pearson chi-square or fisher exact tests for categorical variables were used for comparisons between groups. Wilcoxon rank-sum test was also used to compare the number of episodes before and after ablation All data were analyzed with a statistical package, SAS version 9.2.

Results

We evaluated 58 patients with symptomatic ERS (51 cardiac arrest survivors and 7 syncope). Of the 58, 6 were excluded from the study because of anoxic brain damage after cardiac arrest. The remaining 52 patients (4 females; mean age, 37 ± 14 years) were enrolled into the study (Table 1); clinical characteristics of each patient are also included in the supplemental Table 1. All patients except 1 (who refused ICD) had an ICD for VF therapy; all except 2 patients had frequent VF episodes (ranging from 1 to >150 episodes in the previous 3 months prior to the

procedure). Twenty-two patients had been on quinidine, which was either ineffective or not tolerated in 18 of 22 patients (82%). None of the patients had structural heart disease.

VF Substrates

Of the 52 patients, combined endocardial and epicardial mapping could be performed in 51 patients. One patient had VF storms with frequent VF episodes during the procedure, precluding detailed mapping. In this patient, however, VF triggers were mapped and ablated.

We found two distinct phenotypes (Table 2): 40 patients (Group 1) harbored an arrhythmogenic substrate on the epicardium characterized by fractionated EGMs exhibiting low voltage (<1 mV) and fractionation with prolonged duration (≥70 ms), (Figure 1A). In contrast, 11 patients (Group 2) had inferolateral ERS on their ECG but did *not* have any abnormal EGMs despite detailed epicardial mapping. Group 1 patients were older and more often of male gender than Group 2 patients (mean age 38 vs. 29 years; p=0.051) and 100% males compared to 36% females in Group 2 (p=0.001).

Nineteen percent of the Group 1 patients had SCN5A mutation, but none of the Group 2 patients did. Group 2 had a much higher incidence of J-wave elevation in both inferior and lateral leads than did Group 1 (82% VS. 28%; p =.009). Most Group 1 patients (82.5%) had concomitant Brugada ECG pattern, whereas there were none in Group 2 patients (p<0.0001).

The presence of Brugada ECG pattern subcategorizes Group 1 patients into 2 subgroups (Table 3): Group 1A (N =33) patients had a combination of J-wave pattern (either at the inferior leads, lateral leads or both) and a Brugada ECG pattern (21 spontaneous, and 12 unmasked after sodium channel blocker); Group 1B patients (N=7) had only J-wave pattern. Of significance, sodium channel blockade accentuated the J-wave pattern in inferolateral leads in 6 Group 1A patients (Supplemental Figure 1). VF substrates in Group 1B were more predominantly located

at the inferior RV epicardium (compared to the RVOT/RV epicardium in Group 1A with concomitant Brugada pattern).

Globally in Group 1 (n=40), abnormal fractionated late potentials were present at the epicardium of the RVOT/anterior RV in 38 patients (95%) and at the inferior aspect of the RV in 34 (85%) patients. In addition, 4 (10%) patients had abnormal potentials in the LV epicardium, at the posterior/lateral area (n=2), the apical-septal area (n=1), and the interventricular groove (n=1) (epicardial projection of the LV septum). Only one patient had abnormal endocardial EGMs (at the inferior aspect of the RV close to the tricuspid annulus along with anterior RVOT epicardial substrate).

Group 2 patients (n=11) had no identifiable epicardial or endocardial abnormal depolarization coinciding with the inferolateral J wave. Sodium channel blockade did not lead to aggravation of the J-wave pattern in these patients. Figure 2 shows an example of normal EGMs recorded from endocardium and epicardium of both ventricles. The patient had left Purkinje system as VF triggers. Ablation of these triggering sites was successful. Although VF was inducible prior to ablation, it was not inducible after ablation. The patient had no VF recurrence without antiarrhythmic drug for 7.5 years.

VF Triggers

We identified VF triggers in 14 patients; 12 of the 14 patients (86%) had VF triggers emanating from the Purkinje system: 9 (75%) from the left and 3 from the right Purkinje network, respectively. In the remaining 2 patients, the foci of the PVC VF triggers were at the RV inferior wall in one and left ventricular (LV) posterior wall in the other. An example of a PVC triggering a VF episode during an arrhythmic storm is shown in the Figure 1B & 1C.

VF Drivers: Results of Non-invasive Maps in VF

We performed ECGI non-invasive mapping of VF (2 spontaneous and 30 induced VF) in 32 patients (25 in Group 1, and 7 in Group 2). The mean VF cycle length, measured at 5 second after initiation, was significantly shorter in patients *without* abnormal epicardial signals (157 ± 15 ms in Group 2 vs. 190 ± 10 ms in Group 1, $p<0.001$).

ERS Group 1 patients with late depolarization (n=25):

The distribution of VF driving activities in Group 1 patients (both with or without Brugada ECG pattern) is shown over the 6 compartments on the ventricular surface (Figure 3): 1) anterior RVOT/RV; 2) inferior RV; 3) inferior LV; 4) LV posterolateral; 5) interventricular septum; and 6) interventricular groove. In Group 1 the presence of focal/reentrant drivers, detected by ECGI and abnormal late fractionated EGMs co-localized in the same regions, occurred predominantly at the RV epicardium (100% correlation). Examples of the noninvasive mapping and its correlation with the location of abnormal late-fractionated EGM areas are shown in Figure 4. The drivers in Group 1 JWS patients distributed in the anterior RVOT/RV (region 1) and the RV inferior wall (region 2) in 100% and 88%, respectively (Panel A, Figure 3).

Figure 5 demonstrates a striking similarity between a spontaneous VF episode and induced VF in one of the Group 1A patients. In this patient, the distribution of VF drivers and focal activities not only co-localize with low-voltage late potentials but also is similar between spontaneous and induced VF (Figure 5A). Moreover, the culprit PVC that initiated VF was also located at the same area (right inferolateral RV epicardium) where rotational activities sustain VF were abundant (Figure 5B).

Group 2 patients without late depolarization (n=7):

In contrast to Group 1 patients, Group 2 patients had VF driving activities predominantly located in the inferior ventricular wall, which distributed among three inferior wall regions: 100% at the inferior septum at the interventricular groove (Region 6), 100% at the inferior LV (Region 3), and 60% inferior RV (Region 2) (Panel B, Figure 3).

Catheter Ablation

Forty-three of the 52 patients underwent catheter ablations because of recurrent VF. The remaining 9 patients who did not undergo ablation include 5 Group 2 patients with no identifiable VF substrates, and 4 Group 1 patients who preferred quinidine therapy.

For the 43 patients who underwent catheter ablation, the median number of ablation procedures was 1 (mean 1.4 ± 0.6 procedures); details of each individual patient's ablation and mapping data are also provided in the supplemental Table 2 & 3. Of these patients, 36 were ERS Group 1 with mappable abnormal substrate, 6 were ERS Group 2, and 1 patient had incomplete detailed mapping. Group 2 patients had no identifiable late depolarization abnormalities serving as targets for ablations, but all had identifiable VF triggers mainly in the left posteroinferior Purkinje network (n=5) and only 1 from the right posterior Purkinje network. Ablations at these sites prevented VF recurrence in all. For one patient, who was not classified to any group, had VF trigger from the left posteroinferior Purkinje network ablated successfully and in turn abated the VF storms.

Thirty-one Group 1 patients underwent ablation based exclusively on substrate mapping; 5 had both substrate plus VF trigger ablation. The ablated substrate locations were predominantly at the epicardium of the anterior RVOT/RV (100%) and inferior wall RV (32 of the 36 [89%]). Almost all these patients (n=31; 86%) had ablated substrates in both sites. In only a minority of

the patients, the substrates were also present elsewhere: in the LV posterolateral in 4 (11%) and in the endocardial inferior RV close to the tricuspid valve in 1 patient. The ablation areas were larger (20 ± 6 cm$^{2)}$) than those of Group 2 (4 ± 0.7 cm^2) undergoing VF trigger ablations ($p<0.0001$).

Figure 6 shows an example of abnormal EGM sites from another Group 1B patient who had multiple ICD discharges for VF recurrences. As shown in this figure, the abnormal fractionated late potentials and the VF drivers colocalized in the anterior RVOT, and inferior RV epicardium LV posterior wall apical areas (Figure 6A & B). Ablations at these areas eliminated all fractionated signals, prevented both spontaneous and induced VF and normalized the ER pattern in the ECG of this patient (Figure 6C). Over all, ablations normalized Brugada ECG pattern in all Group 1A patients except one (97%) and resulted in disappearance of ER pattern in 32 of the 39 patients (82%); follow up ECG were missing in 2 patients (Supplemental Table 2).

Pre-ablation inducible VF was present in 32 of 36 (89%) Group 1 and 5 of 6 (83%) Group 2 patients,. After ablation, only 4 of 23 (17%) Group1 re-tested patients had inducible VF ($p < 0.001$); none of the 2 Group 2 patients who had repeat programmed stimulation had inducible VF.

Clinical Outcomes and Complications

Table 4 shows that the effect of catheter ablation on the VF recurrent outcome. After a single procedure. 29 of 43 (67%) patients remained free of VF recurrences without antiarrhythmic medications; the number increased to 39 of the 43 (91%) after the repeat procedure (mean 1.4 ± 0.6 procedures) with the mean follow-up period of 31 ± 26 months from the last ablation ($p <0.0001$). The remaining 4 patients, who had VF recurrences after ablation, had only one ablation session and declined a second procedure based on a drastic reduction of VF episodes.

Only one patient developed a serious complication (hemopericardium). During the follow-up period, all patients who underwent an ablation therapy are alive and well. except for one patient who died from gunshot wounds 3 months after the ablation**. In contrast**, two siblings from Group 2 who did not undergo ablation treatment and were treated developed intractable VF despite quinidine therapy, causing fatal multiorgan failure in one and prompting cardiac transplantation (unfortunately unsuccessful) for the other.

Discussion

We present the first systematic study of mapping and ablation of inferolateral ERS in humans. Key observations are: First, ERS patients express one of the two distinct groups: a) depolarization abnormalities predominantly at the RV epicardium and b) absence of depolarization abnormality areas. Second, late depolarization areas co-localize with VF drivers. Third, these abnormal depolarization areas represent good target sites for ablation. Fourth, ablations at these sites prevent both VF induction and VF recurrences. Fifth, the Purkinje network is the leading underlying electrophysiologic abnormality causing VF in ERS patients devoid of depolarization abnormalities.

Patients with identifiable arrhythmogenic substrate in the epicardium (Group 1) differed from patients without abnormal signals despite extensive epi/endocardial mapping (Group 2): They were older and invariably of male gender (compared to 33% females in Group 2). Also, no Group 2 patients had SCN5A mutations compared to 19% in Group 1. All Group 1 patients who were treated with quinidine failed to respond to the drug, whereas 50% of the Group 2 patients responded to the quinidine.

Learning from our observation that depolarization abnormalities play an important role in the underlying mechanism of the ERS, the term "Early Repolarization" may not be appropriate, because it implies repolarization abnormality as the main mechanism of the syndrome. Thus, we now refer to ERS as JWS.

Electrophysiologic Substrate of JWS

Our current study is also the first in humans to use both invasive detailed epicardial and endocardial mapping and non-invasive mapping studies simultaneously during sinus rhythm and VF. The mapping studies unequivocally demonstrate the presence of abnormal late-depolarization abnormalities in most patients with JWS, particularly in those with coexisting spontaneous or drug-induced BrS. The spatial distribution of these abnormal EGMs is predominantly clustered in the RV epicardium including the RV inferior wall, sometimes in the LV, and very rarely in the RV endocardium. The presence of anterior RVOT/RV substrates confirmed our previous report that these areas are the most common substrate of the BrS, but the incidence of VF substrates in the RV inferior epicardium (86%) in our inferolateral/JWS patients is much higher than that of pure BrS without concomitant inferolateral J wave.[10,11] Four patients also had abnormal areas of EGMs along the posterior and lateral aspect of the LV. The presence of abnormal EGMs in the LV shares some similarity to the observation of late epicardial depolarization associated with structural heart disease and VT[14,15] and supported by computer simulation data that conduction slowing, caused by reduced sodium current in the lateral ventricular myocardium can provoke J-waves which coincide with delayed activation[16]. This dovetails well with our observation that ajmaline accentuated the J-wave pattern in our Group 1 patient supporting the notion that a J wave can be the manifestation of late depolarization located at any part of the right or left ventricles, provided that it occurs late enough to infringe

the terminal QRS complex.[16] Ajmaline may either attenuate or accentuate infero-lateral J-waves[17,18] and one study by Bastiaenen et al suggests that the patients whose J-waves persist or are even accentuated by ajmaline are more likely to have a history of arrhythmic symptoms,[17] like all the patients in our study.

The presence of the conduction delay and late fractionated EGMs in our patients raises the possibility that structural abnormalities too subtle to be picked up by current imaging technologies play a key role in the pathogenesis of JWS. Our group and others have shown that subclinical structural abnormalities of the RVOT epicardium and myocardium constitute VF substrates exhibiting abnormal late-potential EGMs in BrS patients.[19,20] It is therefore likely that a similar phenomenon is present in JWS patients. Furthermore, even though the RV is the dominant site of VF substrates, the LV epicardium in some patients also harbors these substrates. Therefore, one could infer from these findings that a large proportion of diagnosed today with ERS have subclinical fibrosis in both ventricles more easily identifiable in late activated areas like the RVOT and RV inferior wall.

Our finding that the areas with abnormal EGMs co-localize with VF reentrant and focal activities that drive sustained VF, further supports the concept that these areas are VF substrates. VF drivers detected from ECGI non-invasive mapping during VF were 100% concordant with the areas of abnormal late fractionated potentials in the RV epicardium.

However, this is not necessarily true for Group 2 patients with no demonstrable areas with late depolarization abnormalities or fractionated EGMs . The findings that VF cycle length in this group is much shorter than that of Group 1 and that more patients in this Group responded to quinidine suggest that repolarization abnormality plays a major role in the underlying electrophysiologic mechanism of Group 2 JWS patients.

The other important finding in Group 2 patients is that Purkinje network is the main culprit triggering VF. This observation dovetails with ECGI mapping that VF rotors and focal activities are consistently at the septum in Group 2 patients (100%), possibly representing drivers and VF initiators emanating from the Purkinje systems. The other explanation of why reentrant rotors tended to anchor at the septum derives from the study in the rabbit heart and a computer model under the condition of reduced I_{Na} [16, 21]. These show that when the RV is the source of drivers, propagation from the thinner RV has insufficient current to excite the septum and LV, causing the sink-source mismatch and block predisposing the reentry anchored around the septum at the epicardium.[21,22] A similar mechanism has been described for BrS.[21]

Catheter Ablation: An Important Therapeutic Modality

Treatment of life-threatening ventricular arrhythmias of patients with inferolateral JWS is hitherto limited to only quinidine, which is unavailable in most parts of the world[23]. Although a few case reports have shown the benefit of catheter ablation in treating patients with a combined syndrome of BrS and JWS,[24-25] ours is the first and largest study to demonstrate the presence of VF substrates in JWS patients and to define the effective strategy for ablation of JWS. Our study shows that percutaneous catheter ablations are effective in preventing recurrent VF episodes. This is relevant because currently there is no other established treatment for these patients, especially if quinidine is ineffective or not tolerated. Our study suggests that ablation can also be considered as a first-treatment option for cardiac arrest survivors.

Although JWS patients in Group 2 did not have identifiable VF substrates, the majority could undergo successful catheter ablation within the Purkinje network that prevented VF recurrences during long-term follow-up.

Study Limitations

Our findings that the majority of our JWS patients have late depolarization abnormality are possibly due to referral biases, as the patients were often referred for catheter ablation after drug failure, including quinidine, which may be less effective in patients with depolarization abnormality. However, over 60% of our study cohort was from Southeast Asia and did not have access to quinidine; thus, it is unlikely that the patient population was skewed by this form of selection bias.

Many of our patients were highly symptomatic (several had electrical storms) and were referred for ablation as a last resort. Consequently, some patients might not have undergone full detailed mapping because of frequent VF episodes requiring multiple shocks in the laboratory. Additionally, since we did not employ intracardiac ultrasound for visualization of the Papillary muscle, we cannot entirely exclude its role in generating Purkinje potentials that cause VF-triggering PVCs.

Conclusion

Our study demonstrates that electrophysiologic mechanisms underlying JWS are complex. For the first time, we demonstrate that late depolarization abnormalities, predominantly in the RV epicardium, contribute to the underlying mechanism of the syndrome. We have also found that the Purkinje network of both ventricles, especially from the posterior and inferoposterior septal areas of the LV, play an important role in giving rise to VF triggers and initiators. Such areas are important ablation target sites that were successfully ablated in our study, resulting in prevention of recurrent VF episodes. Thus, we show that ablation of the VF substrate sites and/or VF triggers is an effective modality for the treatment of the JWS, and a welcome addition to the therapeutic armamentarium of this syndrome.

Further study to delineate the role of repolarization disorder and its interplay with late depolarization substrate will be needed. A randomization study to compare the treatment between quinidine and ablation is also warranted. Based on our findings, any symptomatic JWS patients should be considered for ablation treatment.

Source of Funding

This work is supported by: The National Research Council of Thailand (Grant number 2558-114) & Grants in Aid from Bumrungrad hospital Bangkok, Thailand and Medtronic Inc, USA; the National Research Agency (ANR-10-IAHU04-LIRYC), the European Research Council (FP7/2007–2013 grant agreement number 322886, SYMPHONY), and Leducq Transatlantic Network of Excellence grant. (RHYTHM) 16CVD02.

Disclosures

Dr. Nademanee receives research grants and royalty from Biosense Webster Inc. He also receives a research grant from Medtronic Inc. The authors affiliated to IHU Liryc disclose a Research Collaboration on noninvasive electrocardiographic imaging between Medtronic and the IHU Liryc.

References

1. Shipley RA, Hallaran WR. The four-lead electrocardiogram in two hundred normal men and women. Am Heart J 1936;11:325-345.
2. Haïssaguerre M, Derval N, Sacher F, Jesel L, Deisenhofer I, de Roy L, Pasquié JL, Nogami A, Babuty D, Yli-Mayry S, et al. Sudden cardiac arrest associated with early repolarization. N Engl J Med 2008;358:2016-2023.
3. Tikkanen JT, Anttonen O, Junttila MJ, et al. Long-term outcome associated with early repolarization on electrocardiography. N Engl J Med 2009;361:2529-2537.

4. Rosso R, Glickson E, Bellhassen B, Katz A, Halkin A, Steinvil A, Viskin S. Distinguishing "benign" from "malignant early repolarization": The value of the ST-segment morphology. Heart Rhythm 2012;9: 225-229.
5. Antzelevitch C, Yan GX. J wave syndromes. Heart Rhythm 2010;7:549-558.
6. Nademanee K, Wilde AAM. Repolarization Versus Depolarization Defects in Brugada Syndrome: A Tale of Two Different Electrophysiologic Settings? JACC Clin Electrophysiol 2017;3:364-366.
7. Kakihara J, Takagi,M, Hayashi Y, Tatsumi H, Doi A, Yoshiyama M. Radiofrequency catheter ablation for treatment of premature ventricular contractions triggering ventricular fibrillation from the right ventricular outflow tract in a patient with early repolarization syndrome. Heart Rhythm Case Rep 2016;2:342-346.
8. Nogami A. Mapping and ablating ventricular premature contractions that trigger ventricular fibrillation: trigger elimination and substrate modification. J Cardiovasc Electrophysiol 2015; 26: 110-115.
9. Haïssaguerre M, Extramiana F, Hocini M, Cauchemez B, Jais P, Cabrera J, Farre G, Leenhardt A, Sanders P, Scavee C, et al. Mapping and ablation of ventricular fibrillation associated with long-QT and Brugada syndromes. Circulation 2003;108:925-928.
10. Nademanee K, Veerakul G, Chandanamattha P, Chaothawee L, Ariyachaipanich A, Jirasirirojanakorn K, Likittanasombat K, Bhuripanyo K, Ngarmukos T. Prevention of ventricular fibrillation episodes in Brugada syndrome by catheter ablation over the anterior right ventricular outflow tract epicardium. Circulation 2011;123:1270-1279.
11. Nademanee K, Hocini M, Haïssaguerre M. Epicardial Substrate Ablation for Brugada syndrome. Heart Rhythm 2017;14:457-461.
12. Ramanathan C, Ghanem RN, Jia P, Ryu K, Rudy Y. Noninvasive electrocardiographic imaging for cardiac electrophysiology and arrhythmia. Nat Med 2004;10:422-428.
13. Wang Y, Cuculich PS, Zhang J, Desouza KA, Vijayakumar R, Chen J, Faddis MN, Lindsay BD, Smith TW, Rudy Y. Noninvasive electroanatomic mapping of human ventricular arrhythmias with electrocardiographic imaging. Sci Transl Med 2011;3(98): 98ra84.
14. Haïssaguerre M, Hocini M, Cheniti G, et al. Localized Structural Alterations Underlying a Subset of Unexplained Sudden Cardiac Death. Circ Arrhythm Electrophysiol 2018;11:e006120.
15. de Bakker JM, Wittkampf FH. The pathophysiologic basis of fractionated and complex electrograms and the impact of recording techniques on their detection and interpretation. Circ Arrhythm Electrophysiol 2010;3:204-213.
16. Meijborg VM, Potse M, Conrath CE, Belterman CN, De Bakker JM, Coronel R. Reduced sodium current in the lateral ventricular wall induces inferolateral J-Waves. Front Physiol 2016;7:365.
17. Bastiaenen R, Raju H, Sharma S, Papadakis M, Chandra N, Muggenthaler M, Govindan M, Batchvarov VN, Behr E. Characterization of early repolarization during ajmaline provocation and exercise tolerance testing. Heart Rhythm 2013;10:247–254.
18. Roten L, Derval N, Sacher F, Pascale P, Wilton S, Scherr D, Shah A, Pedersen MEF, Jadidi A, Miyazaki S, Knecht S, Hocini M, Jaïs P, Haïssaguerre M. Ajmaline attenuates electrocardiogram characteristics of inferolateral early repolarization. Heart Rhythm 2012;9:232–239.

19. Nademanee K, Raju H, De Noronha S, Papadakis M, Robinson L, Rothery S, Makita N, Kowase S, Boonmee N, Vitayakritsirikul V, et al. Fibrosis, connexin 43, and conduction abnormalities in the Brugada syndrome. J Am Coll Cardiol 2015;66:1976-1986.
20. Coronel R, Casini S, Koopmann TT, Wilms-Schopman F, Verkerk AO, de Groot JR, Bhuiyan Z, Bezzina CR, Veldkamp MW, Linnenbank AC, et al. Right ventricular fibrosis and conduction delay in a patient with clinical signs of Brugada syndrome: a combined electrophysiological, genetic, histopathologic, and computational study. Circulation 2005;112:2769-2777.
21. Park CJ, Arevalo HJ, Trayanova NA. Arrhythmogenesis in Brugada Syndrome: role of ventricular structure. Biophys J 2011;100:435a.
22. Qing L, Li W, Efimov IR. The role of dynamic instability and wavelength in arrhythmia maintenance as revealed by panoramic imaging with blebbistatin vs. 2, 3-butanedione monoxime. Am J Physiol Heart Circ Physiol 2012;302:H262-269
23. Viskin S, Wilde AA, Guevara-Valdivia ME, Daoulah A, Krahn AD, Zipes DP, Halkin A, Shivkumar K, Boyle NG, Adler A, Belhasen B, Schapachnik E, Asrar F, Rosso R. Quinidine, a life-saving medication for Brugada syndrome, is inaccessible in many countries. J Am Coll Cardiol 2013;61: 2383–2387.
24. Lim PC, Nademanee K, Lee EC, Teo WS. Epicardial ablation utilizing remote magnetic navigation in a patient with Brugada syndrome and inferior early repolarization. Pacing Clin Electrophysiol 2018;41:214-217.
25. Krothapalli SM, Giudici M, Demetroulis E, Sigurdsson G, Goldsmith G, Mazur A. Abnormal epicardial electrophysiologic substrate in patients with early repolarization pattern and reduced left ventricular systolic function: A report of two cases. Heart Rhythm Case Rep 2017;3:422-426.

Table 1. Clinical characteristics of the study patients

Number of Patients	52
Age	37 ± 14 (median 35) years
Gender (M/F)	48 (92%) /4 (8%)
Symptoms	Aborted cardiac arrests/VF = 45 (87%) Syncope = 7 (13%)
Family History	18 (35%)
Brugada ECG Pattern	33 (65%) spontaneous (N=21, 64%), drug induced (N=12, 36%)
Location of J-Point Elevation	Inferior wall only = 30 (58%) Inferolateral = 19 (36%) Lateral wall only = 3 (6%)
Distribution of Patients According to Total Number of VF Episodes on ICD*	No episode = 2 (4%) 1-4 episodes = 12 (24%) 5-9 episodes = 7 (14%) 10-20 episodes = 13 (25%) >20 episodes = 17 (33%)
SCN5A Mutation (only 32 had completed genetic study	4 of 32 (13%)
Racial Distribution	Southeast Asian = 26 (49%) Japanese = 6 (12%) Chinese = 1 (2%) Caucasians = 17 (33%) African American = 2 (4%)
Quinidine Failure/Intolerance	18 of 22 treated with quinidine (82%)

The number of patients enrolled into the study from each study site: Chulalongkorn University & Pacific Rim Electrophysiology Research Institute = 31; University of Bordeaux = 15; University of Tsukuba = 5 ; St. George's University Hospital = 1.

*1 patient did not have an ICD

Table 2. Comparison of Group 1 versus Group 2 with Respect to Clinical and Electrophysiologic Characteristics

	Group 1: Late Depolarization. (n=40)	Group 2: J wave without late Depolarization. (n=11)	P value
Age	38.4 ± 13	29.3 ± 16	0.051
Female Gender	0 (0%)	4/11 (36%)	0.001
Presence of BrS ECG	33 (82.5%)	0 (0%)	<0.0001
Locations of J-Wave Elevation	26 inferior only (65%) 11 inferolateral (28%) 3 lateral only (7%)	2 inferior only (18%) 9 inferolateral (82%)	0.009
Family History	14 (35%)	4 (36%)	1.000
SCN5A Positive	4 of 21 (19%)	0 of 11 (0%)	0.272
VF Storms	21 (54%)	5 (41%)	0.679
VF Cycle Length (msec)	205 ± 20	147 ± 19	<0.0001
Location of Drivers	Right ventricle (100%) Inferior RV Epi (88%)	Inferior ventricular wall (100%): both interventricular groove and LV inferior wall	-----
#Treated with Quinidine/ # Response to Quinidine	14/0 (0%)	8/4 (50%)	<0.0001
# Treated with Ablation	36 (95%)	6 (55%)	0.015
Ablation Location	Predominantly epicardium of the RV	Left Purkinje system for VF triggers	
Ablation areas	20 ± 6 cm^2	4 ± 0.7 cm^2	<0.0001
Number of Ablation (Mean ± SD)	1.4 ± 0.65 (range 1-3; median 1)	1.2 ± 0.41 (range 1-2; median 1)	0.289
Complications of Ablation	1 hemopericardium	None	------

Table 3. Comparison between Group 1A versus Group1B with respect to clinical and electrophysiologic characteristics including ablation Variables.

	Group 1A: JWS-Late Depolarization with Combined ERS & BrS (N =33)	Group 1B: JWS-Late depolarization with ERS only (N =7)	P value
Age	39.3 ± 12	34.3 ± 15.7	0.352
Locations of J-wave Elevation	20 inferior only 10 inferolateral 3 Lateral only	5 inferior only 2 inferolateral	0.687
Family History	10 (30.3%)	4 (57.1%)	0.214
SCN5A Positive	4 out of 15 (27%); 19 pending genetic study	0 out of 6 (0%); 1 pending genetic study	0.281
VF Cycle length (Mean ± SD)	201 ± 18	183 ± 12	0.05
Locations of Electroanatomic Substrates	Anterior RVOT/RV Epi (100%); Inferior RV epi (91%); Posterolateral LV (3%).	Inferior RV Epi (100%); Anterior RVOT/RV Epi (60%); Apical & Posterior LV Epi (20%).	
Location of Drivers	RVOT/Ant RV (100%), Inferior RV Epi (88%)	RVOT/anterior RV epicardium (100%), Inferior RV epicardium (100%)	
Number of patients underwent Ablation	32 (97%)	4 (57%)	0.1
Ablation Locations	Predominantly epicardium of the RVOT/anterior RV and RV inferior wall.	Predominantly epicardium of the anterior RV and RV inferior wall.	
Ablation areas (cm^2) Mean ± SD	20.4 ± 6.2	18.6 ± 6.2	0.547
Number of Ablation Mean ± SD Median (IQR)	1.3 ± 0.7 1 (1 – 2)	1.0 ± 0.8 1 (0 – 2)	0.333 0.485

Table 4. Effects of Ablation on VF Recurrence in 43 patients who underwent the procedure.

	No VF	**1-4 VF Episodes**	**5-9 VF Episodes**	**10-20 VF Episodes**	**> 20 VF Episodes**
Before Ablation	0 (0%)	8 (19%)	7 (16%)	12 (28%)	16 (37%)
After 1st Ablation	29 ** (67%)	11 (26%)	3 (7%)	0 (0%)	0 (0%)
After last Ablation*	39** (91%)	4 (9%)	0 (0%)	0 (0%)	0 (0%)

* After last Ablation or a follow-up period of 31 ± 26 months after the last Ablation.
** $p < 0.001$

Figure Legends

Figure 1. An Example of Depolarization Abnormality and VF Trigger in One of The Group 1B Patients. Figure 1A shows a CARTO-merge map, from a patient with J-waves in the inferior leads but no Brugada pattern (Figure 1B & 1C), who presented with VF storms triggered by PVCs from the right Purkinje network. The cardiac computed tomography of the patient's heart is merged with the electroanatomic maps of the RV and LV epicardium recorded during electrophysiologic studies. Areas in the CARTO-merge are color-coded according to the local EGM voltage, ranging from red (lowest local signals with ≤ 0.5 mV amplitude) to magenta (highest voltage, i.e., ≥ 1.5 mV). The insets display the EGMs recorded from the NaviStar-ThermoCool catheter at various sites of RV and LV epicardium. The voltage map and the representative bipolar tracings are shown. Note that the EGMs in the inferior and inferolateral aspects of the RV are of low amplitude, are fractionated, and have prolonged duration (>70 ms) with depolarization delayed beyond the end of the QRS complex corresponding with the prominent notched J-Wave in the simultaneously recorded ECG lead III. M1-M2 = denote bipolar recordings from the distal pole of the ablation catheter. Figure 1B displays 12-lead ECG showing prominent J-Waves in the inferior leads and intracardiac recordings of the ablation distal (ABLd) and proximal pairs (ABLp) and the right ventricular apex (RVA) from the same patient of the Figure 1A. Note that there are 2 morphologic PVCs; the first PVC emanated from the LV and had superior axis and right bundle branch block morphology and did not trigger VF. The second PVC is the VF trigger and has inferior axis with QRS morphology of deep Q or S waves across the precordial leads and has the focus from the right Purkinje network. The Figure 1C shows the recording of the ablation catheter at the RV Purkinje system at the RV septum. The

prominent notched J-wave is clearly present in Lead 3 (arrow). The ablation distal pair records a very small Purkinje potential (PurJ) preceding the ventricular EGM, which has slight prolonged duration of 75 ms during sinus rhythm. This was the earliest site of the PVC with the sharp PurJ immediately before ventricular EGM (-45 ms before the QRS onset) that has the identical morphology as the VF trigger in Figure 1B. Ablations at this site abated the VF storm.

Figure 2. An Example of a CARTO Map from One of The Group 2 Patients. The admission EKG from a 52-year-old male Group 2 patient with aborted sudden death and normal heart shows inferolateral J-waves of high amplitude (Panel A). The ECG recorded 2 days after the index event is normal (Panel B). Panel C shows a composite biventricular map of epicardium and LV endocardium. Note that despite extensive epicardial mapping, there are no late depolarization abnormalities.

Figure 3. The Distribution of VF Drivers. Panel A (N =25) and Panel B (N = 7) show distributions of focal activity and reentrant circuits over both ventricle for Group 1 patients and Group 2 patients respectively. We divide epicardial surface of both ventricle into 6 Regions: 1) anterior RVOT/RV; 2) inferior RV; 3) inferior LV; 4) posterolateral LV; 5) interventricular septum; and 6) interventricular groove. Note that In Group 1, the driver activities predominantly at the RV (RVOT (100%, Region 1) and inferior RV (88%, Region 2). In contrast, Group 2 has their driver activities predominantly in the inferior wall (100%, Regions 6 & 3).

Figure 4. Correlation Between Areas Harboring Late Fractionated Potentials and VF Drivers. Figure 4A shows an ECGI map and abnormal fractionated late potentials from the RV

epicardial recording from one of a Group 1A patient with multiple VF episodes who had J-Wave elevation in the inferolateral leads at baseline (Supplemental Figure 2) and the Brugada ECG pattern in the right precordial leads after ajmaline. The numbers on the ECGI map represent the number of rotations at each point on the heart as recorded at 5 seconds of a VF episode. The colored hexagons represent the number and location of epicardial focal breakthroughs. The ECGI maps in the middle panel show AP view on the top, and caudal view of the inferior aspect of both ventricles at the bottom. The right and left panels show the bipolar EGMs and unipolar EGM recorded from the distal and proximal pair-electrodes and the distal electrode of the ablation catheter at the inferior aspect of the RV, which shows fractionated late potentials co-localizing with the colored areas that have >16 rotation count within these areas. The color-scale bars on the top left of the ECGI map shows the scale of the number of focal activities (range 1-4; orange to red) and the scale of the number of rotational activities (range from 1 [yellow] to 16 [red] on the lower left. Panoramic view of these reentrant and focal activities is shown in Supplemental Video 1. Figure 4B shows abnormal fractionated EGMs recorded from the decapolar catheter positioned at the RVOT, where multiple focal activities in this area are shown with the colored hexagon representing the number and location of epicardial focal breakthrough. The 3 distal pairs of decapolar, DecaN1,2, DecaN 3,4 & DecaN 5,6, show fractionated late potentials beyond QRS complex and prolonged duration (120 msec) of the bipolar recordings and abnormal unipolar recordings of the corresponding electrodes (DecaD-Deca5) mimicking Brugada ECG pattern in the V2, these abnormal potentials corresponding with the J-Wave in V2-ICS3 . In Figure 4C, the left panel shows the ajmaline -12 lead EKGs at baseline and after ablation; ajmaline unmasked the Brugada ECG pattern and slightly accentuated the ER pattern in the inferior leads. Both Brugada and ER patterns disappeared after ablation. The right panel (A-

E), shows a composites of ECG tracing and intracardiac recordings from various sites of the RV epicardium before (pre) and after (post) ablation. In the middle is the CARTO electroanatomic map with a Univue plus Cartomerge of the RV epicardium displaying abnormal EGMs areas in the anterior RVOT/RV epicardium (red dots) and RV inferior epicardium (Orange dots) where ablations were performed. Note that ablations drastically reduced in the fractionated EGM amplitude with disappearance of the mid and terminal complex of the fractionated signals recorded before the ablation, suggesting that the RF energy eliminated the intramyocardial substrate site below the epicardial surface. V1 ICS3 = lead V1 at the ICS3; V2 ICS3 = lead V2 at ICS3; ABLd = Ablation distal pair; ABLp = Ablation proximal pair; ABL uni = Ablation unipolar from the distal electrode. Pre = pre-ablation; Post = post-ablation. The white dots represent right atrioventricular junction and Tricuspid annulus; the brown dots represent late fractionated potentials with an amplitude > 0.9 mV, the red dots represent the late fractionated potentials with an amplitude between 0.5-0.9 mV and the blue dots late fractionated potentials with an amplitude < 0.5 mV.

Figure 5. A Comparison Between the Simultaneous VF Episode and the Induced VF. Figure 5A shows the distribution of VF rotational and focal activities are similar and located at the same areas. The top left panel compares the ECGI maps of the simultaneous and that of induced VF episodes in one of the Type 1A patients. Both had VF drivers located predominantly and extensively on the RV epicardium at the RV inferolateral, RVOT/RV and infero-apical area. These VF drivers also colocalized with fractionated late potentials as shown in the tracings that display ECG Lead 3 displaying prominent notch J-wave with the timing that coincide with these late potentials. Each symbol (*, **, μ, ¶, Ω) on both ECGI maps marks the area that exhibits late

fractionated potentials as shown in the corresponding tracing with the same symbol. The description of the color-scale bars on the left side of the ECGI map is the same as in the Figure 4A. Figure 5B shows the ECGI (displaying in the isochronal activation map) of both sporadic PVC (Left panel) and PVC that triggered VF (Right Panel). The map clearly shows the figure of 8 reentrant ventricular beats at the right inferolateral RV where rotational figure of 8 activities also were located during spontaneous VF. The color-scale bar on the left side of the ECGI map represent the activation time in msec from early (red) to late (blue). The phase map of these reentrant activities is shown in the Supplemental video 2.

Figure 6. Another Example of Colocalization of VF Drivers and Late Depolarization Abnormality. Figure 6A shows recordings from a Group 1B patient who had frequent VF episodes and late depolarization abnormalities in both RV and LV ventricular epicardium. The left panel shows the caudal view of three maps of both ventricles: Top: CARTO merge map during sinus rhythm; Middle: ECGI map during VF , (its phase map is shown in the bottom). Note that the abnormal EGMs and VF drivers co-localize in the same areas. The movie of the VF driver rotation appears in Supplemental Video-3. The right panel shows the ECG lead II, V1 ICS3 and V2 ICS3 and the bipolar and unipolar recordings from the Lasso catheter (20 electrodes) placed at the posterior LV epicardium closed to the basal aspect of the interventricular groove. Note the J-Wave in Lead II coincedes with the low voltage late-fractionated potentials recorded from all bipolar pairs from the lasso catheter. Figure 6B (from the same patient) shows the antero-posterior (AP) view of the CARTO-merge and ECGI maps and the bipolar and unipolar EGMs recorded from the ablation catheter at the RV inferior epicardium (arrow). The movie of the phase map of the RV drivers and focal activity appears in

Supplemental Video 4. Figure 6C (from the same patient) shows normalization of the ER pattern in the inferolateral leads after ablation; both pre- and post- ablation ECGs were recorded after after administration of 50 mg ajmaline, showing no evidence of Brugada ECG pattern).

A

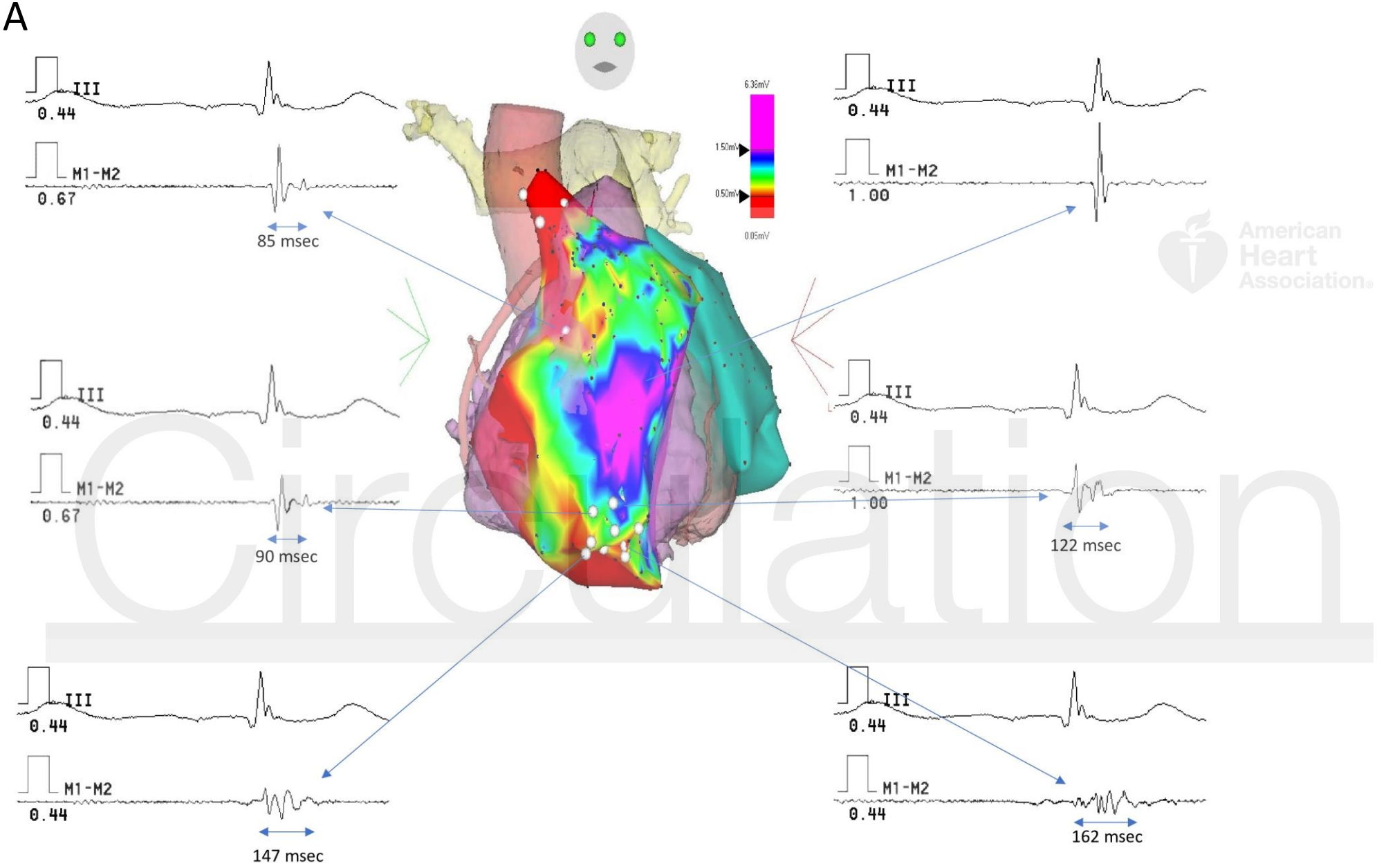

B

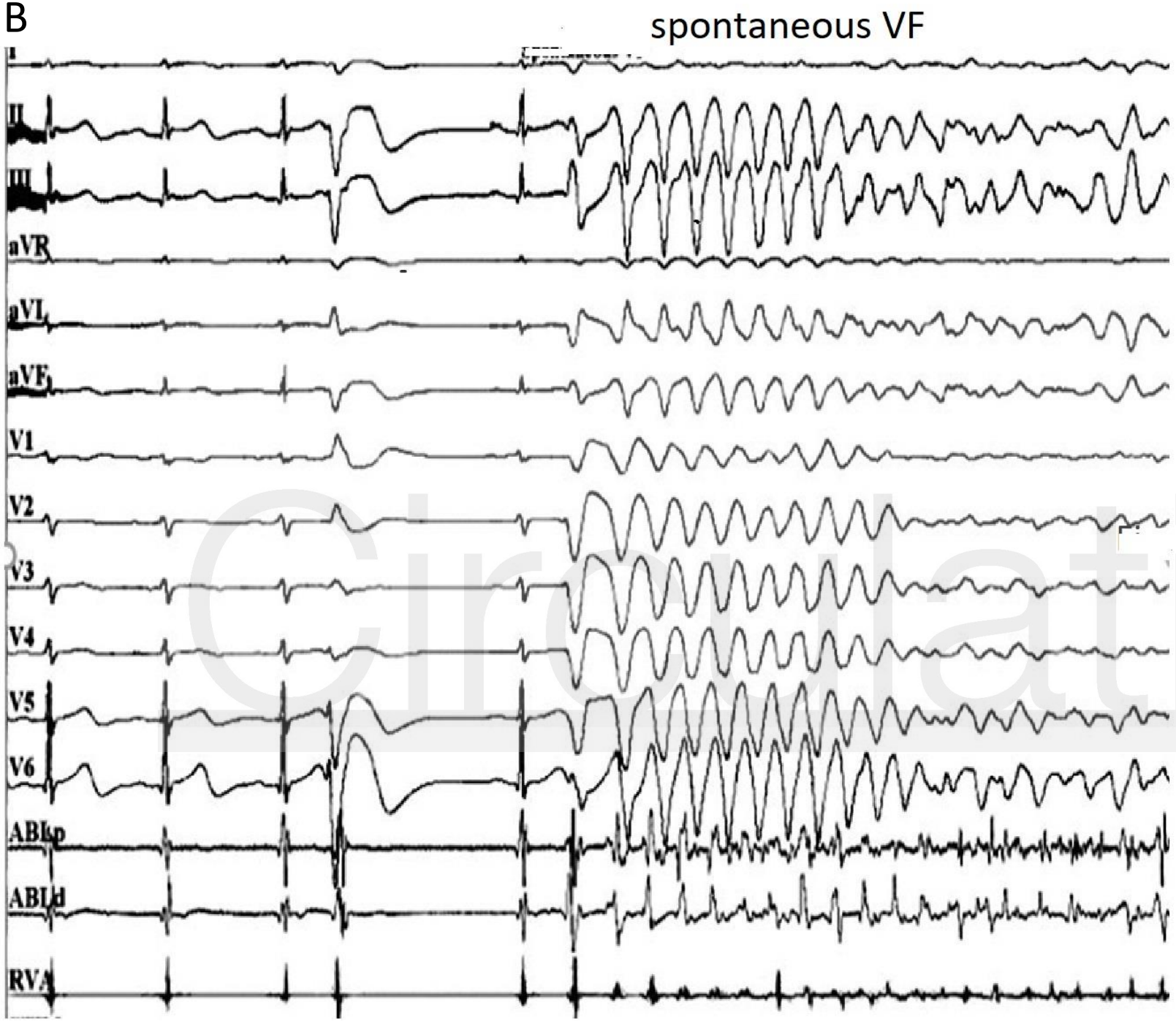

C

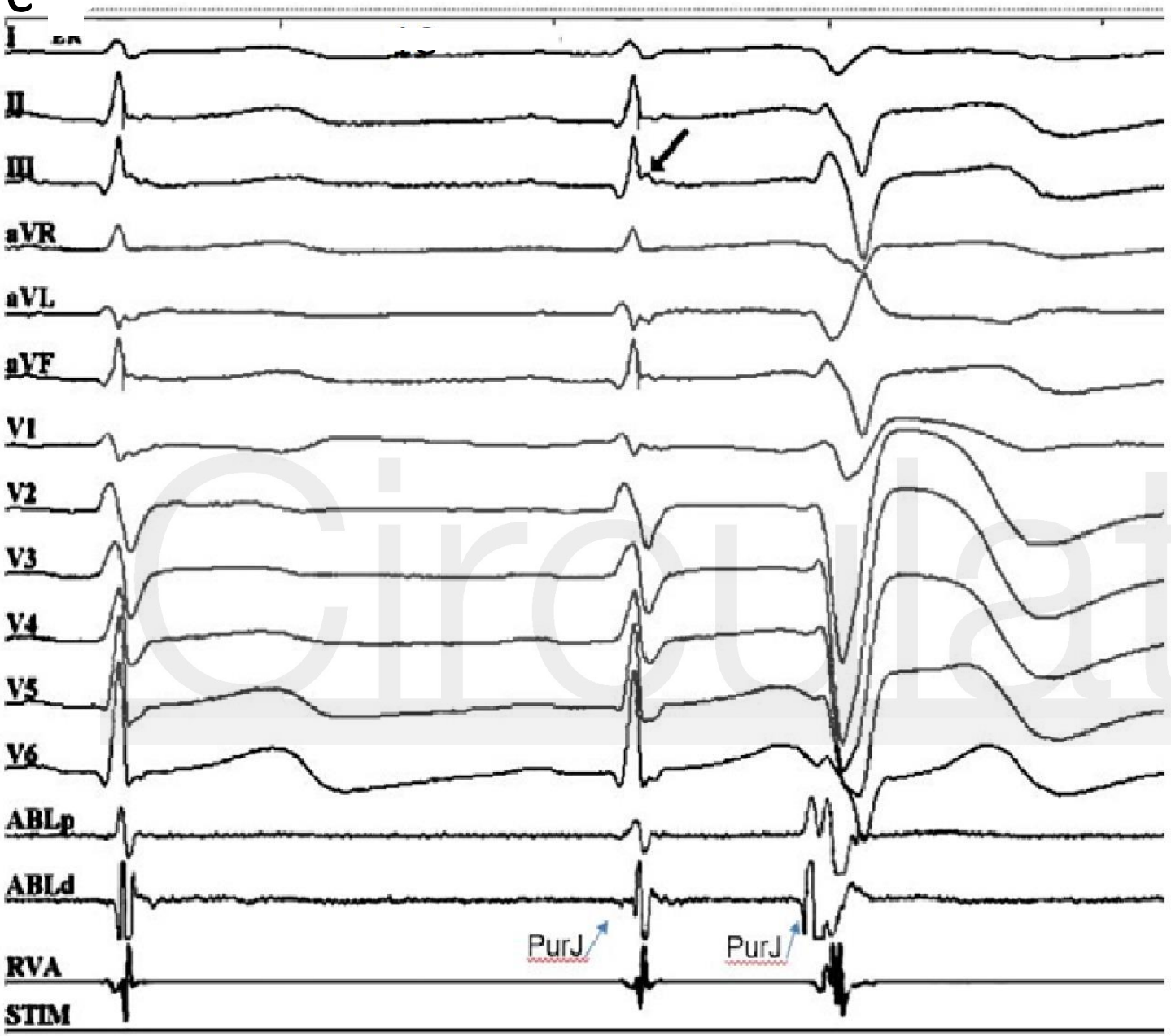

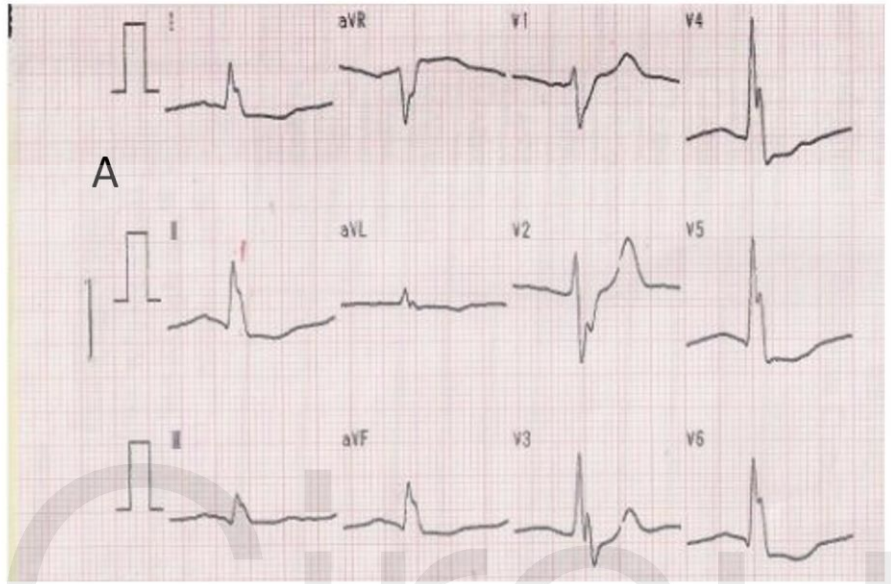

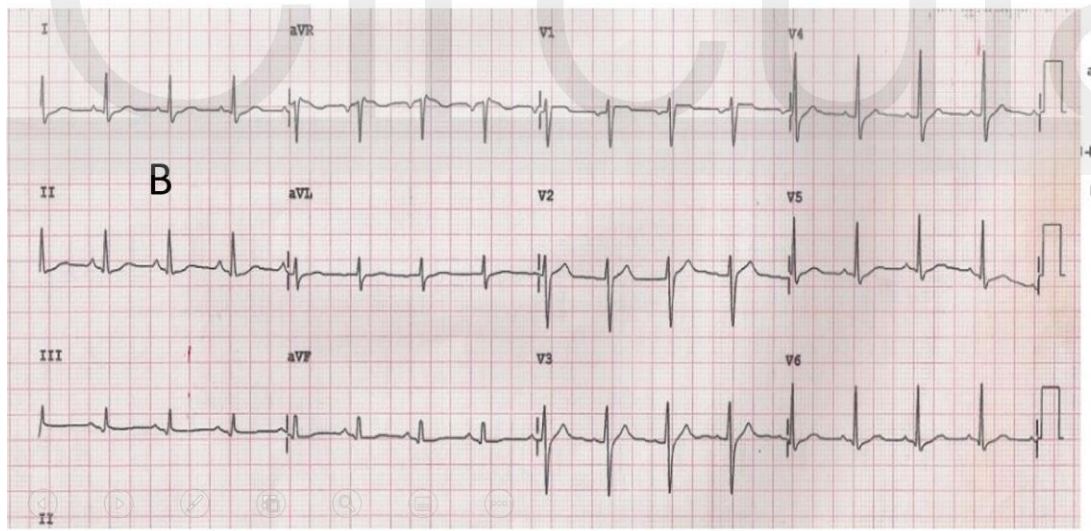

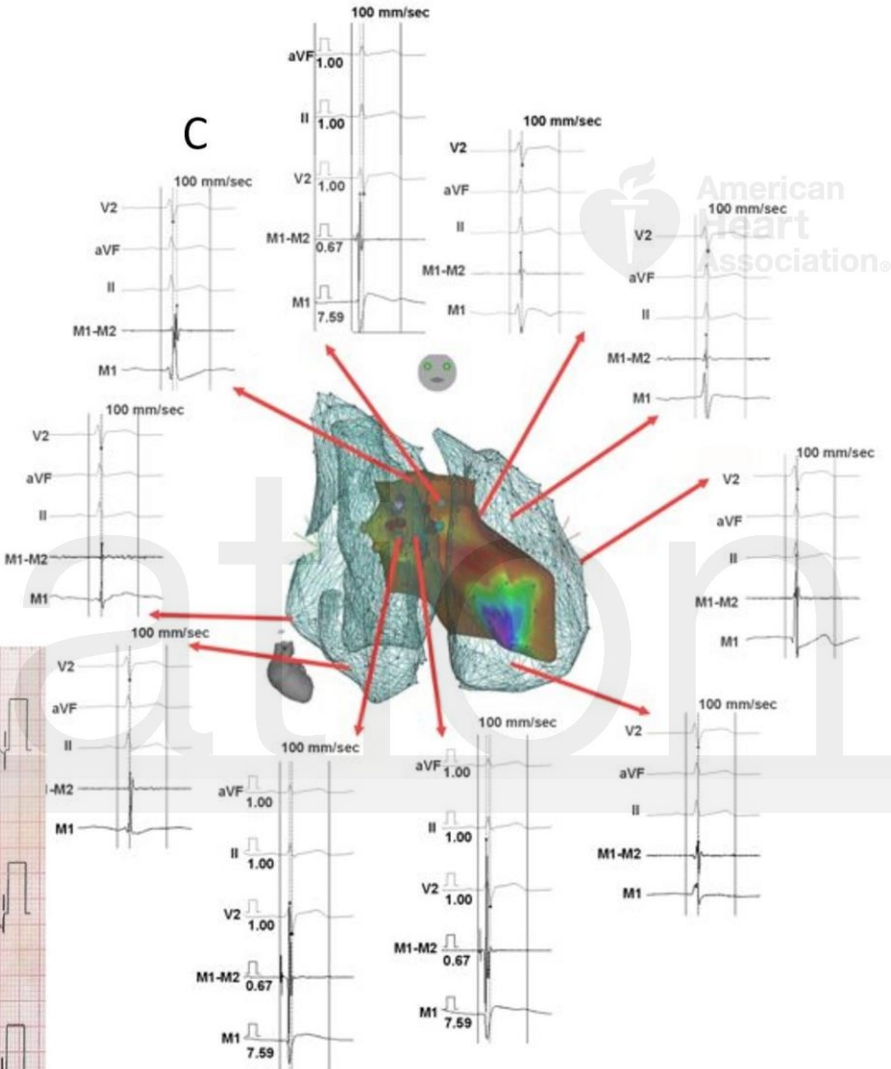

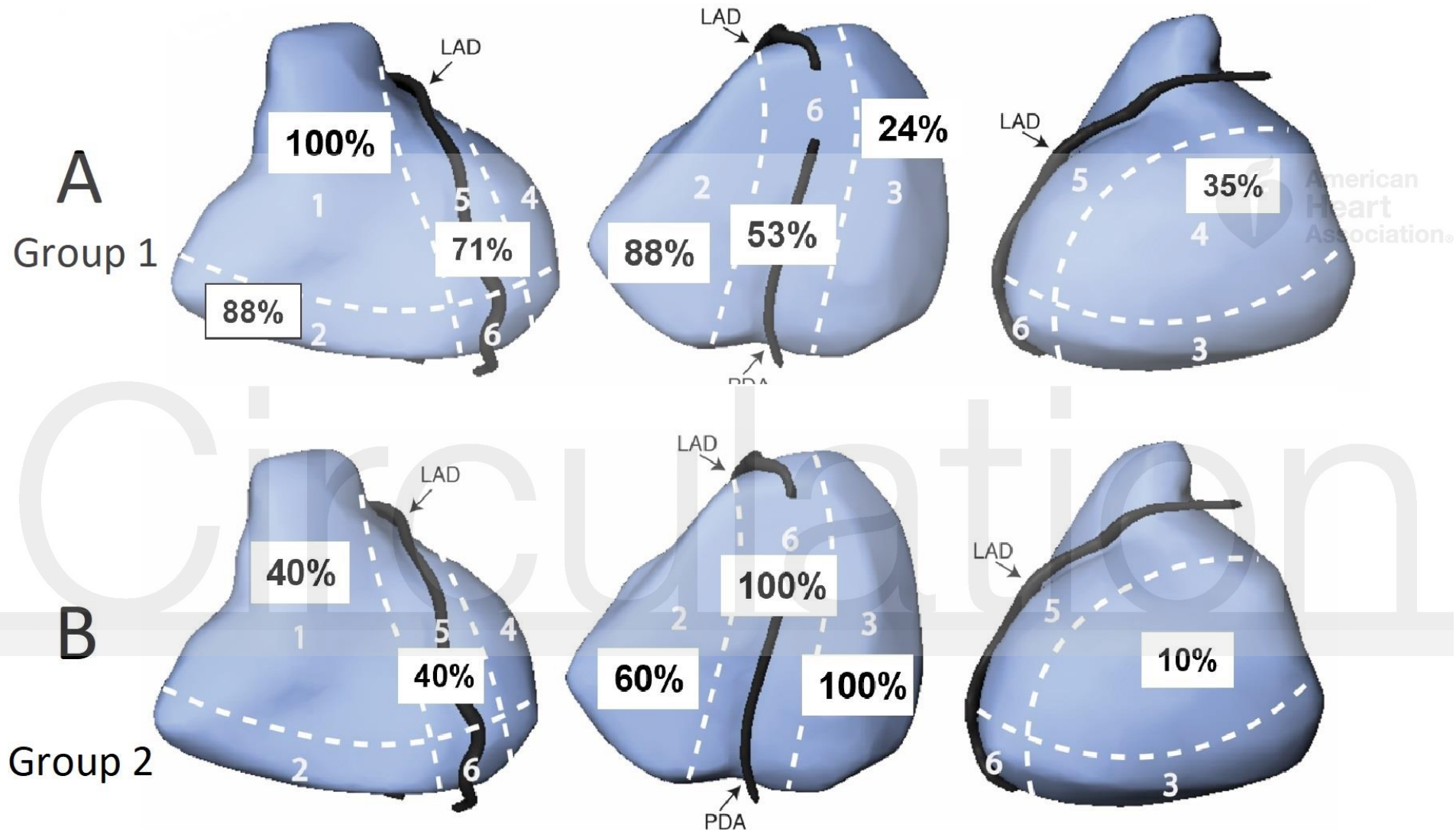

A

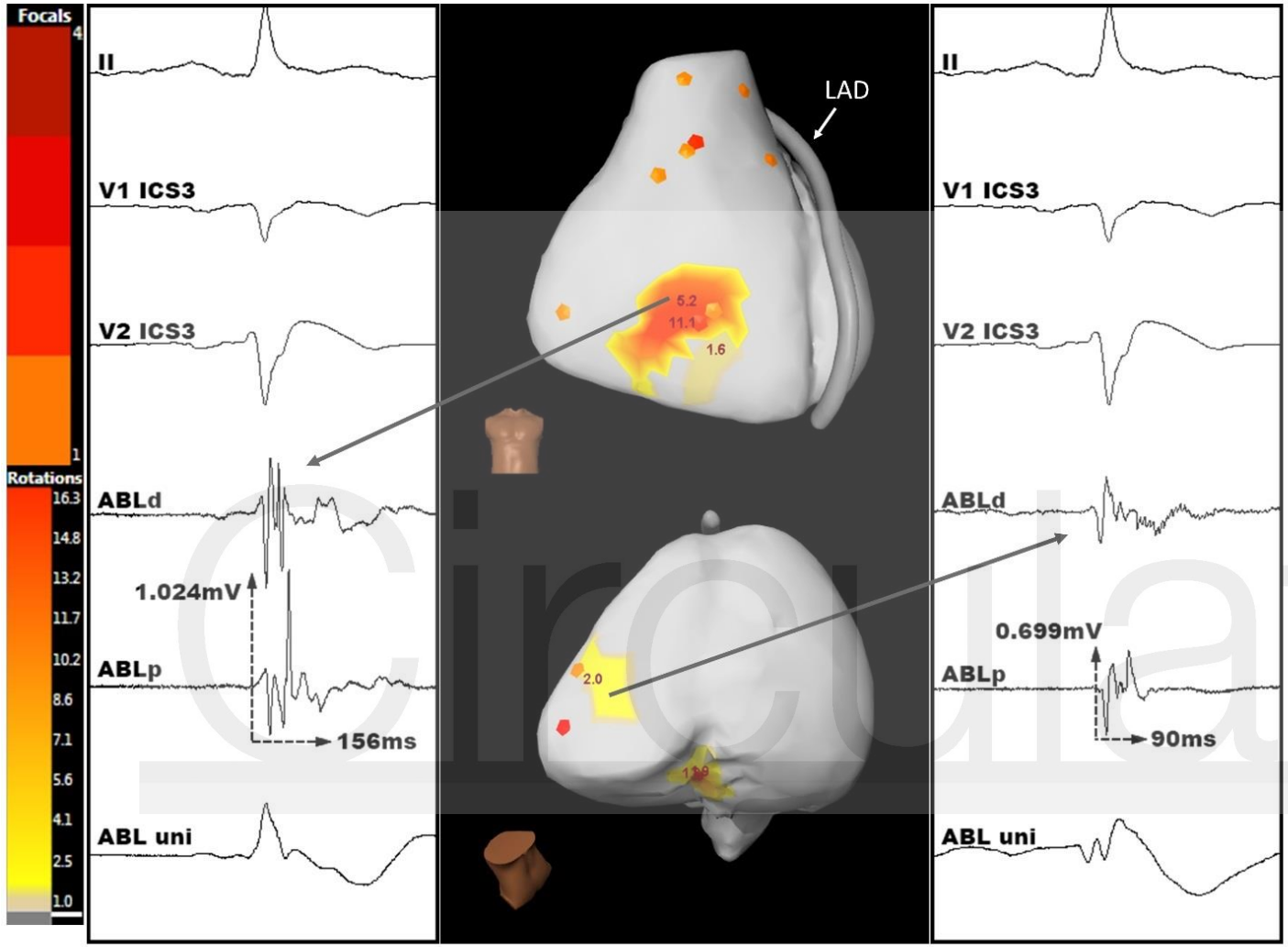

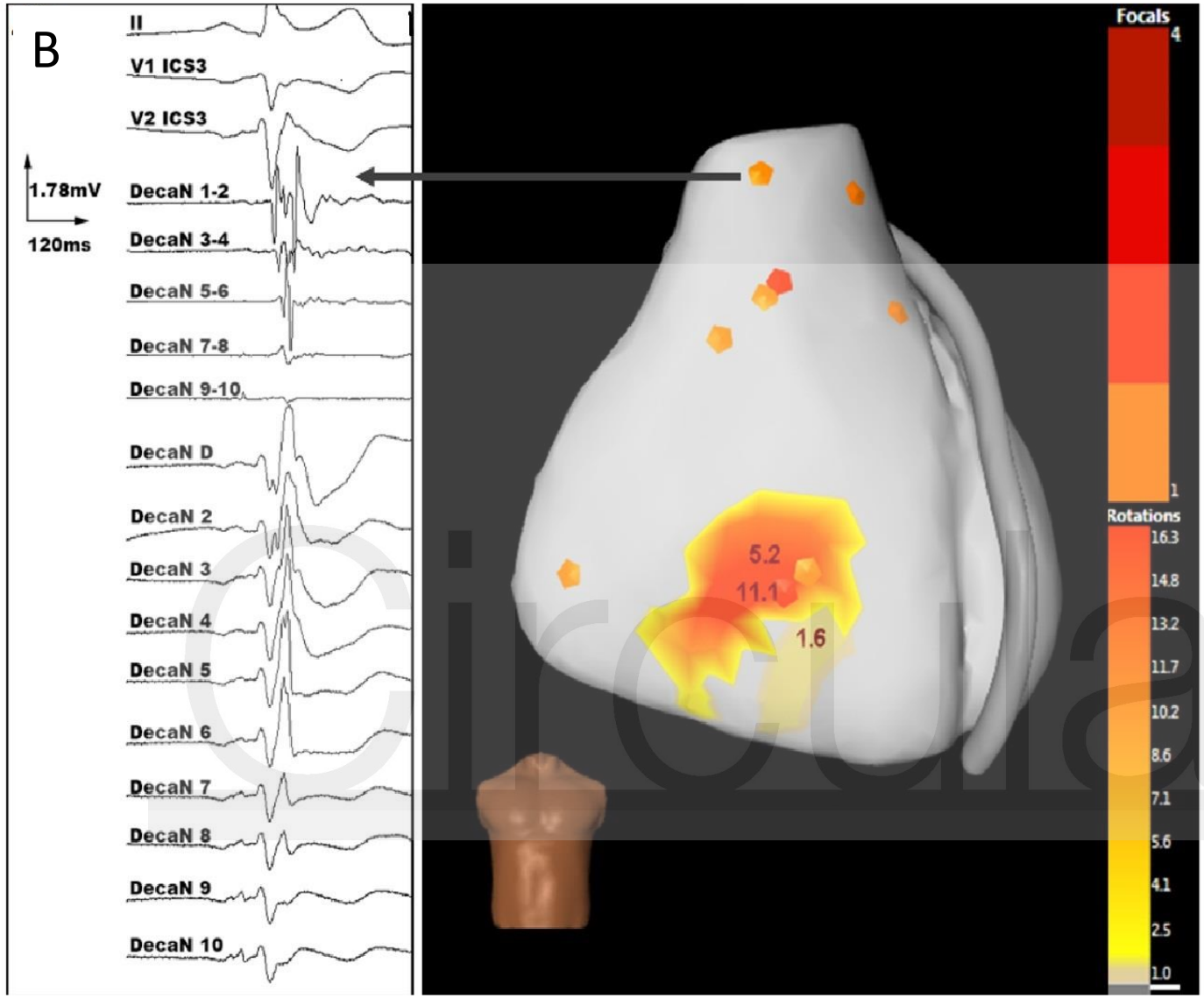

C

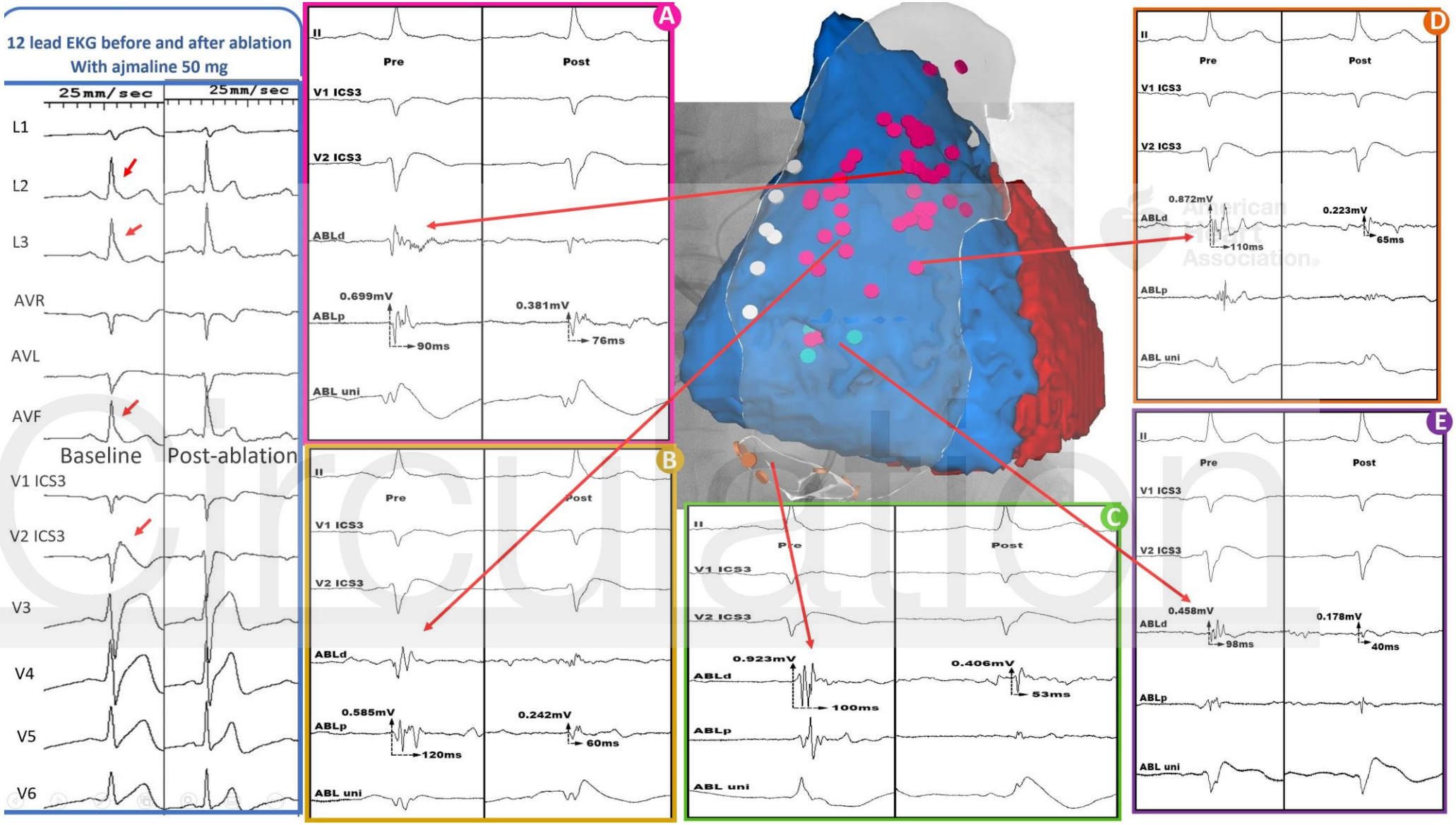

A

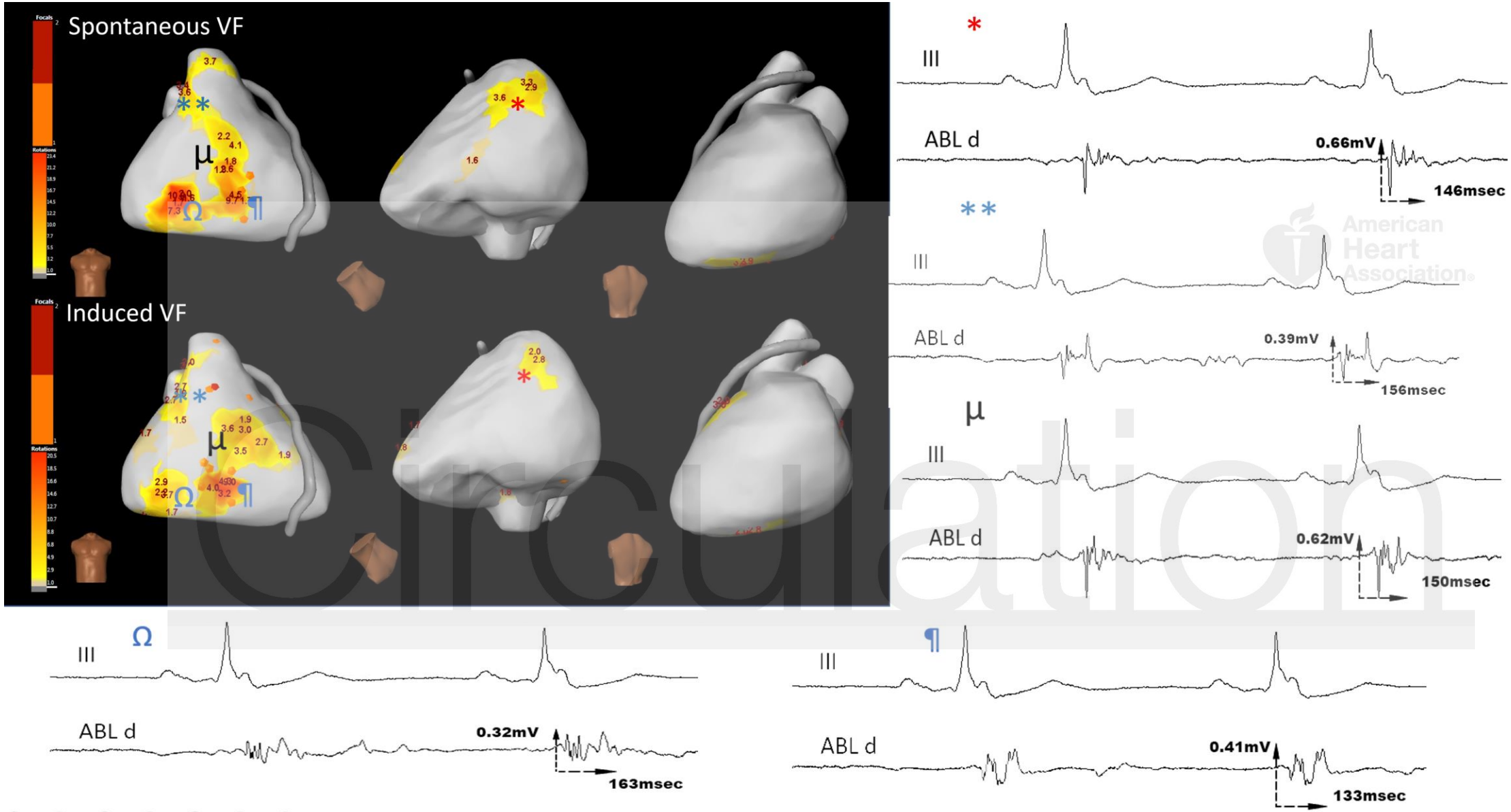

B

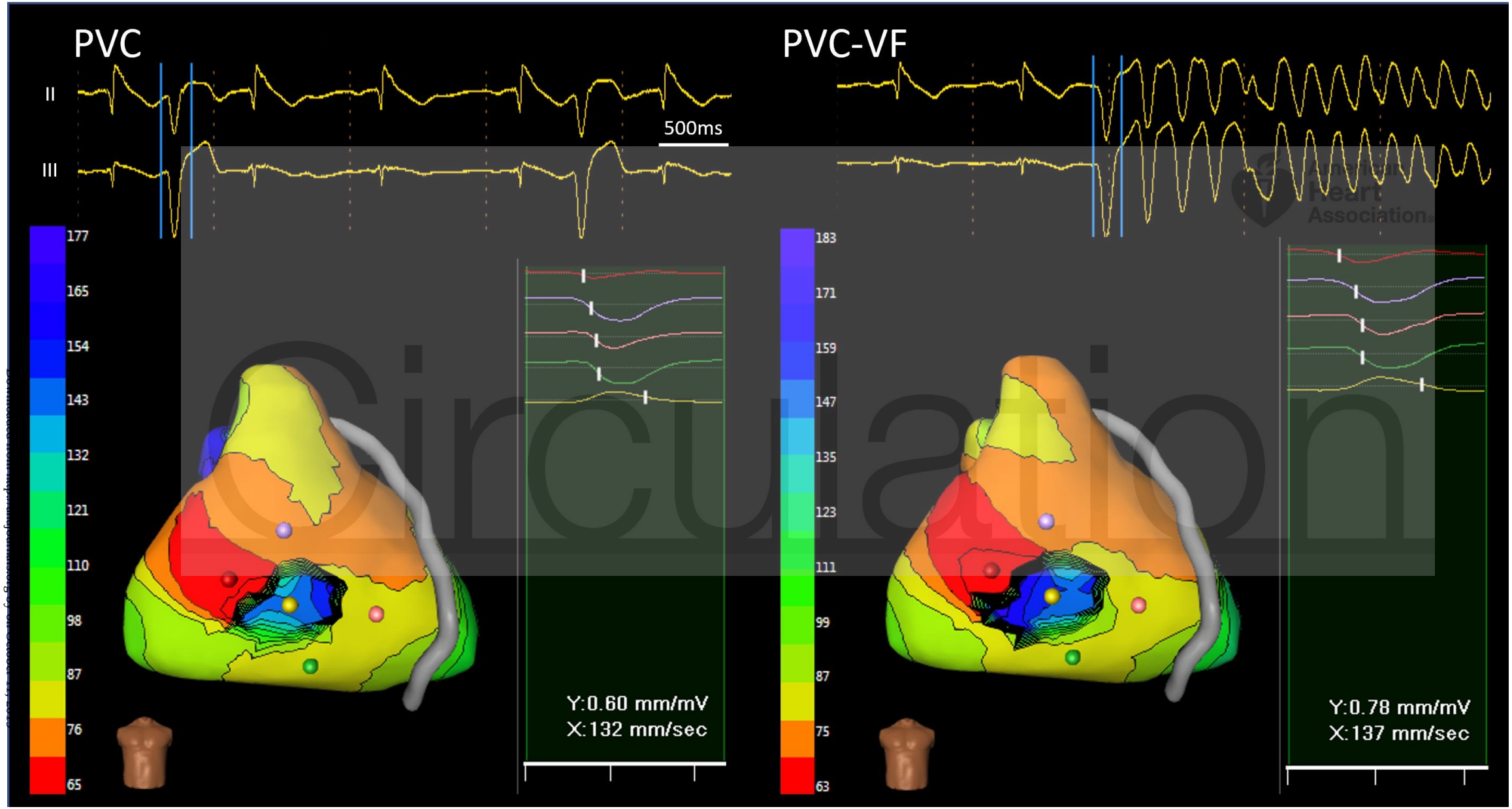
PVC
II
III
500ms
177
165
154
143
132
121
110
98
87
76
65
Y:0.60 mm/mV
X:132 mm/sec
PVC-VF
183
171
159
147
135
123
111
99
87
75
63
Y:0.78 mm/mV
X:137 mm/sec

A

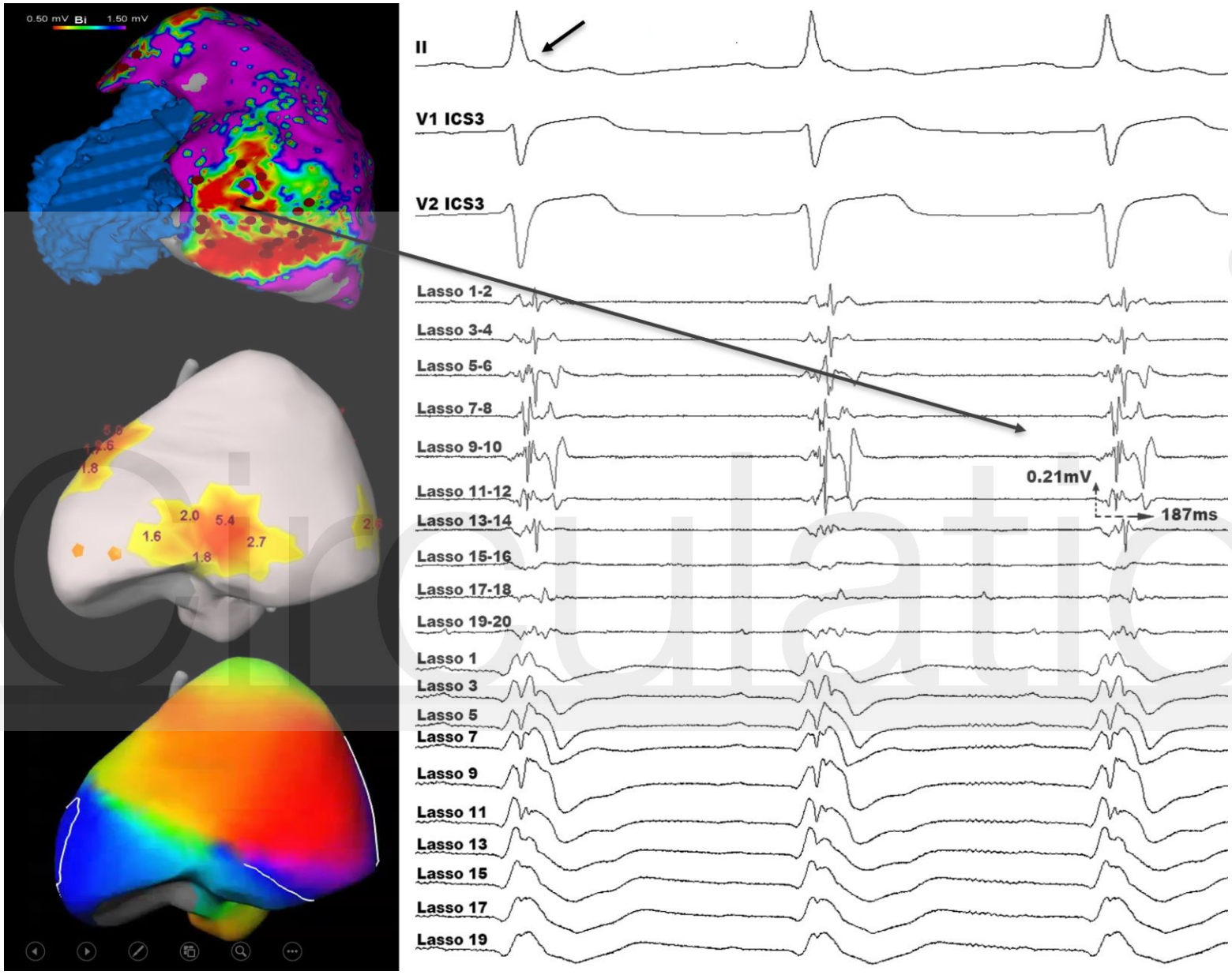

B

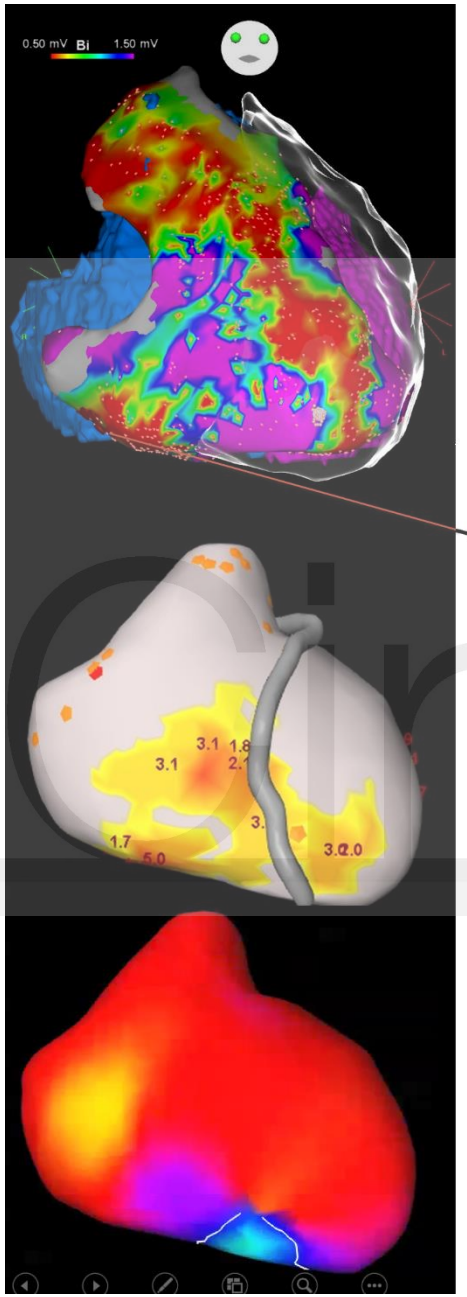

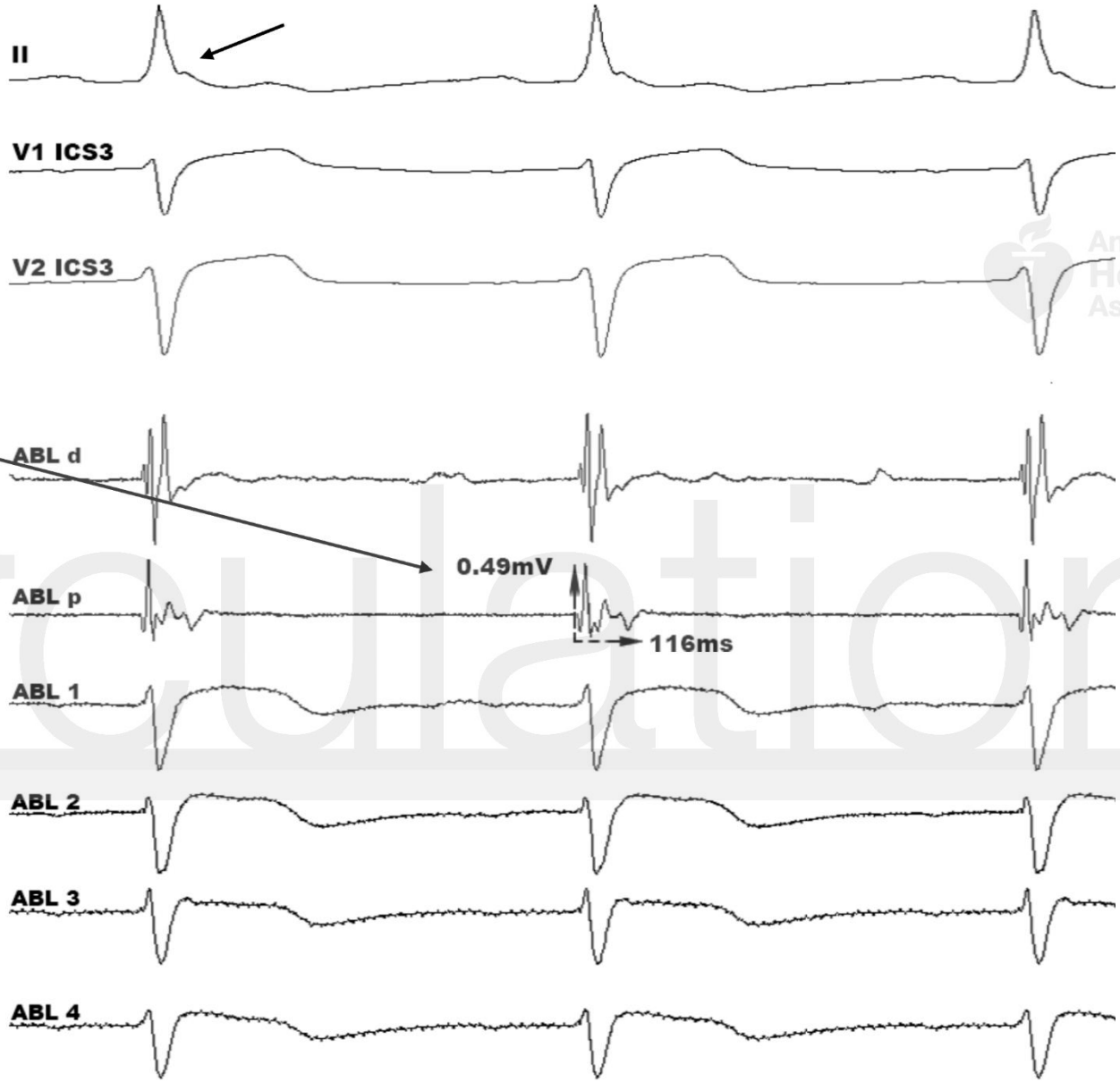

C